

## Electrochemical Synthesis of Asymmetric Gold–Silver Iodide Nanoparticle Composite Films

Mahnaz El-Kouedi, Marie L. Sandrock,  
Carolyn J. Seugling, and Colby A. Foss, Jr.\*

Department of Chemistry, Georgetown University,  
Washington, D.C. 20057

Received June 9, 1998

Revised Manuscript Received September 17, 1998

Nanocomposite materials have become the focus of great interest due to their multiple applications in both electronic and optical devices.<sup>1</sup> This work deals with nanoscopic metal and semiconductor heterojunctions embedded in a dielectric matrix. The nanoscopic size of the particles leads to enhanced optical properties,<sup>2,3</sup> while embedding them in a matrix improves the stability and handling of the material.<sup>1</sup> Many researchers are working in this field and are using polymer matrices, high-temperature glasses, porous glasses, and sol–gel derived glasses as embedding materials. One of the most difficult tasks is controlling the size, shape, and orientation of the particles. The use of anodic aluminum oxide (AAO) as a template material has been developed by the groups of Martin<sup>4</sup> and Moskovits<sup>5</sup> and has been used for the synthesis of organic and metal microtubules and particles.<sup>6–8</sup> Anodic aluminum oxide films have very regular and uniform pore sizes that have also been used for the fabrication of nanowires of CdS.<sup>5</sup>

Also of recent interest is the assembly of metal–semiconductor heterojunctions within the dielectric matrix. For example, cadmium chalcogenides on nickel substrates have been synthesized in commercially available anodic aluminum oxide.<sup>9</sup> Due to the large pore diameters of the commercial AAO, the resulting metal structures would not exhibit strong plasmon resonance extinction in the visible spectrum, nor would quantum confinement effects associated with the semiconductor be evident. Using smaller particles, some groups have electrodeposited particles of Cu–CuO in dielectric materials which exhibit exciton formation.<sup>10</sup>

In this paper we report the results of our first efforts to prepare gold–silver iodide heterojunction rods in anodic alumina hosts whose pores are ca. 30 nm in diameter. Our interest in these heterojunction structures are manifold. First, gold rods prepared in such template hosts are known to show strong plasmon

resonance bands in the visible spectrum,<sup>8</sup> and the optical constants of silver iodide have been well-documented.<sup>11</sup> Thus, this system serves as a convenient model for comparison with the predictions of simple scattering and effective medium type theories.<sup>6</sup> Second, the enhanced local fields arising from the gold phase may be expected to enhance the third-order nonlinear optical properties of the confined semiconductor phase.<sup>12</sup> Finally, the inherent asymmetry of the Au/AgI particles is expected to lead to a nonzero second-order electric susceptibility.

The template synthesis of aluminum oxide was performed using the procedure developed by Martin et al.<sup>4,6</sup> Aluminum foil (99.999% pure) was anodized in a 6% sulfuric acid bath maintained at a temperature of 0 °C for 14 h at 20 V. The aluminum oxide film was then detached using a 5% voltage reduction technique. This procedure yields porous films of ca. 50 μm thickness and pores of ca. 30 nm diameter. The aluminum oxide was then sputtered with a 30–40 nm layer of silver.<sup>13</sup> A three-electrode cell was used for the DC deposition of the silver and gold. The Ag-sputtered oxide was the working electrode. A silver–silver chloride electrode served as the reference and a Pt mesh served as the counter electrode.<sup>14</sup> The first step in the synthesis of the Au/AgI composite was the electrodeposition of a silver base. At least 3 C of silver was deposited over a 3.14 cm<sup>2</sup> area to ensure that the subsequent gold deposition occurs deep in the film where the pore structure is well-defined.<sup>15</sup> The silver was deposited at –0.6V vs SSCE from a silver thiocyanate plating solution. Varying amounts of gold were then deposited at –0.9 V vs SSCE from an Au(I) plating solution. The desired amount of silver for the conversion was then deposited, and the composite films were left overnight to soak in water. This soaking is an important step because it serves to remove excess silver ions from the pore channels that would otherwise precipitate out as AgI when the films are exposed to KI solutions.

The conversion of the second Ag phase to AgI was performed using a modified technique adapted from Rao et al.<sup>16</sup> An aqueous potassium iodide solution (0.10 M) was added to the cell and the potentiostat was set to +0.1 V vs SSCE until all of the uppermost silver layer had been oxidized to silver iodide, which deposits inside the pores close to the gold surface. The silver to silver iodide conversion can be performed at many different positive potentials. At higher potentials the conversion occurs more rapidly, but the AgI deposits appear more granular in TEM images. Finally, the silver base was removed by placing the sample in concentrated nitric acid. The film was then washed with deionized water

\* Corresponding author.

(1) Beecroft, L. L.; Ober, C. K. *Chem. Mater.* **1997**, *9*, 1302.  
(2) Wang, Y. *Acc. Chem. Res.* **1991**, *24*, 133.  
(3) Sipe, J. E.; Boyd, R. W. *Phys. Rev. A* **1992**, *46*, 1614.  
(4) Martin, C. R. *Chem. Mater.* **1996**, *8*, 1739.  
(5) Routkevitch, D.; Bigioni, T.; Moskovits, M.; Xu, J. M. *J. Phys. Chem.* **1996**, *100*, 14037.  
(6) Foss, C. A.; Hornyak, G. L.; Stockert, J. A.; Martin, C. R. *J. Phys. Chem.* **1994**, *98*, 2963.  
(7) Brumlik, C. J.; Martin, C. R. *J. Am. Chem. Soc.* **1991**, *113*, 3174.  
(8) Martin, C. R. *Science* **1994**, *266*, 1961.  
(9) Klein, J. D.; Herrick, R. D., II; Palmer, D.; Sailor, M. J.; Brumlik, C. J.; Martin, C. R. *Chem. Mater.* **1993**, *5*, 902.  
(10) Switzer, J. A.; Hung, C.-J.; Bohannon, E. W.; Shumsky, M. G.; Golden, T. D.; Van Aken, D. C. *Adv. Mater.* **1997**, *9*, 334.

(11) Berry, C. R. *Phys. Rev.* **1967**, *161*, 848.  
(12) Wang, Y.; Herron, N. *J. Phys. Chem.* **1991**, *95*, 525.  
(13) Using Anatech Hummer 10.2 sputtering system.  
(14) The cell is degassed and attached to an EG&G Princeton Applied research potentiostat/galvanostat model 273A. Potentials are referenced against a Ag/AgCl electrode.  
(15) The ends of the aluminum oxide pores tend to be damaged and branched, especially toward the barrier side (side closest to the aluminum).  
(16) Jaya, S.; Rao, P. T.; Rao, P. G. *J. Appl. Electrochem.* **1988**, *18*, 459.

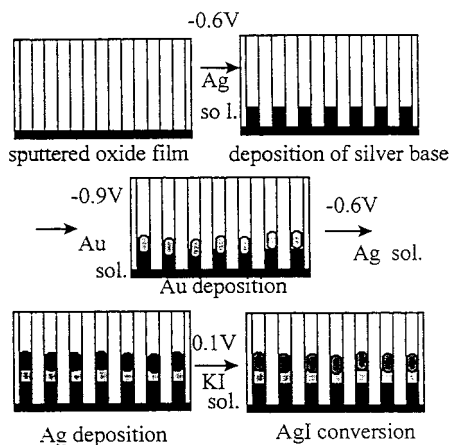


**Figure 1.** Electrochemical synthesis of asymmetric Au-AgI nanoparticle composite films.

and left to dry. The Ag/AgI particle synthesis is summarized in Figure 1.

To evaluate the completeness of the conversion of silver to silver iodide, the oxidation of the second layer of silver was performed using chronoamperometry. The chronoamperometric experiments involved an initial potential of  $-0.4$  V with a step to  $0.2$  V, where the Ag to AgI conversion can take place. The resulting oxidative current was monitored for 5 min, after which it reached the background level. The area under the current-time plot represents the number of atoms of silver oxidized, and was found to be, within experimental error, equal to the number of silver atoms electrodeposited in the second layer. The chronoamperometric studies demonstrate that we have quantitative conversion of silver to silver iodide and that the gold layer acts effectively as a plug to prevent the underlying silver base from being oxidized. It should be noted that low deposition levels of gold lead to incomplete sealing of the pore; chronoamperometry experiments thus show that the silver on both sides of the gold layer is converted to AgI.

Preliminary characterization of the composites was performed using linear absorption spectroscopy and transmission electron microscopy.<sup>17</sup> Figure 2 is a TEM image of  $0.3$  C of Au/ $0.5$  C of AgI in aluminum oxide.<sup>18</sup> In the TEM images, the nanoparticles are rodlike and show no perceivable boundary between the gold and silver iodide regions. Thus the silver iodide and the gold appear to be in direct contact forming one long rod inside the pore. Significantly, TEM images of samples containing only  $0.3$  C of gold also show rodlike structures but have significantly shorter lengths.<sup>19</sup> However, it should be noted that AgI structures in porous alumina are brittle and more susceptible to damage during the microtoming than are the gold segments. Thus, the distribution in the Au/AgI particle lengths as seen in the TEM images is larger than previously seen for template-synthesized Au rods.<sup>20</sup> Finally, the number

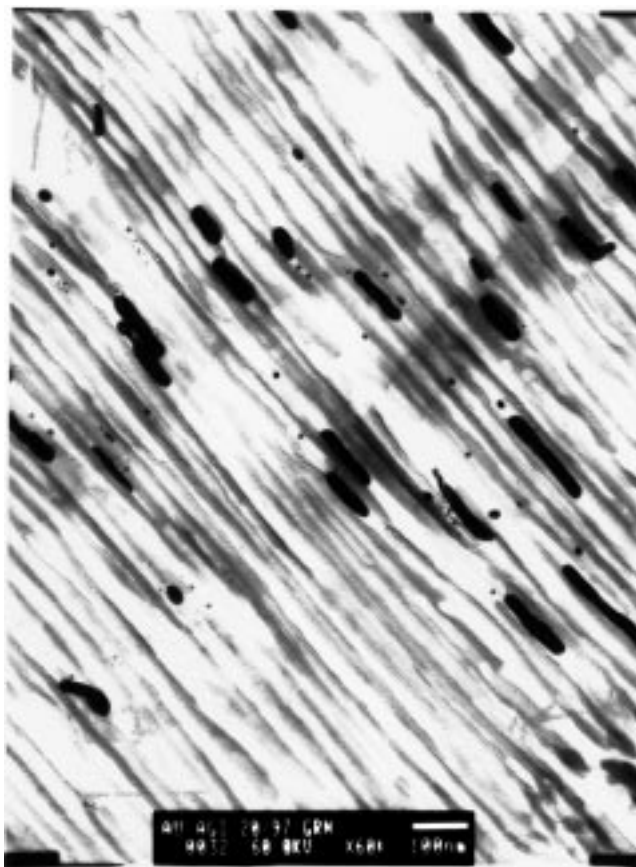


**Figure 2.** Transmission electron microscope image of  $0.3$  C of Au/ $0.5$  C of AgI in aluminum oxide.

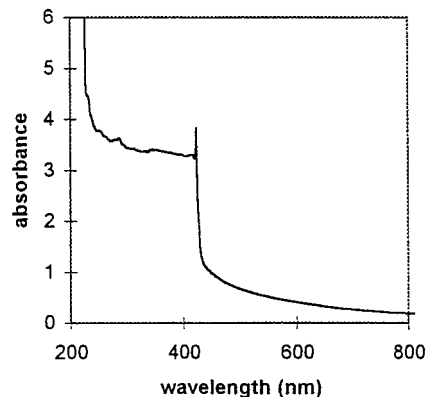


**Figure 3.** Spectrum of AgI in anodic aluminum oxide, exhibiting a strong exciton peak. The spectrum was taken at room temperature and pressure using a Hitachi U-3501 spectrophotometer.

density and distribution in the positions of the particles in the porous host are similar to that seen in TEM images of Au/porous alumina composites discussed previously and arise from the nonuniform lengths of the silver rod foundations.<sup>6</sup>

For comparison purposes, we have also prepared AAO films containing only AgI particles (no Au component). Figure 3 depicts a spectrum of the AgI nanoparticles in the AAO taken at room temperature.<sup>21</sup> The spectrum

(17) Samples are embedded in resin and microtomed to a  $80$  nm thickness.

(18) A sample containing  $0.3$  C of Au denotes  $0.3$  C of gold deposited over a  $3.14$  cm<sup>2</sup> area.

(19) Al-Rawashdeh, N. A. UV/Visible and Surface Enhanced Infrared Studies of Polyethylene/Oriented Gold Nanoparticle Composite Films: The Effect of Gold Particle Size, Shape and Orientation, Ph.D. Thesis, Georgetown University Department of Chemistry, 1996; Chapter 3.

(20) Al-Rawashdeh, N.; Sandrock, M. L.; Seugling, C.; Foss, C. A., Jr. *J. Phys. Chem. B* **1998**, *102*, 361.

(21) All spectra were taken using a Hitachi U-3501 spectrophotometer.

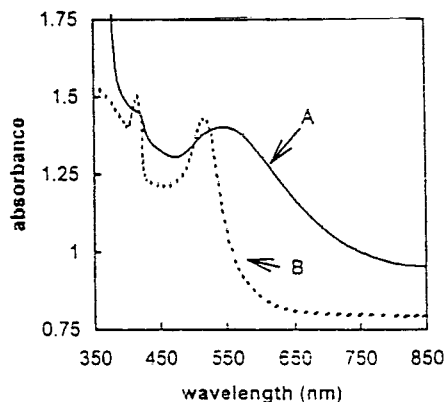


**Figure 4.** Spectrum of  $0.095 \text{ C/cm}^2$  Au and  $0.239 \text{ C/cm}^2$  AgI in aluminum oxide: (a) experimental and (b) simulated using Maxwell-Garnett theory where the two materials are noninteracting. The volume fractions  $f$  and screening parameters  $\kappa$  for the metal and semiconductor are  $f = 0.05$ ,  $\kappa = 1.54$  for Au and  $f = 0.08$ ,  $\kappa = 1.45$  for AgI. The path length was 450 nm.

shows a strong peak at 421 nm which has been identified as an exciton band.<sup>11</sup> Extrapolation of the band edge to baseline yields a band gap energy ( $E_g$ ) of ca. 2.87 eV (430 nm). This spectrum is consistent with the bulk AgI room-temperature spectra reported by Berry.<sup>11</sup> The  $E_g$  value estimated from Figure 2 is close to the 2.82 eV value of bulk AgI reported by Ageev.<sup>22,23</sup>

Figure 4 (curve A) depicts a spectrum taken of the Au/AgI in AAO. We observe the plasmon resonance band of the gold and the band edge of the silver iodide. While the determination of  $E_g$  for the AgI component is not straightforward in this case, the position of the band edge is similar to that of AgI particles prepared in AAO without a contacting Au phase. Interestingly, the strong exciton peak is absent.

The absence of the exciton peak may be interpreted in two ways. First, one might conclude that the electrochemical conversion of the Ag phase to AgI resulted in small crystallites rather than a continuous

phase. Berry's study showed that the exciton peak is absent for 15 nm diameter particles. However, neither the experimental spectra of AgI particles in AAO nor the TEM images of the Au/AgI particles in AAO support this interpretation. The second explanation would be that the contact between the AgI semiconductor and Au metal phases leads to energy transfer and lifetime damping of the exciton peak.<sup>24</sup>

Plasmon resonance peaks have been studied in detail in this lab,<sup>20</sup> and their dependence on particle shape and orientation have been explained in terms of small particle limit scattering or effective medium theory. For the Au/AgI particle composite, the Au plasmon resonance band appears broader and red-shifted relative to those of AAO template-synthesized Au particles of similar dimensions.<sup>19,20,25</sup> For comparison, curve B in Figure 4 is the simulated spectrum using Maxwell-Garnett theory for a simple composite in which the gold and silver iodide phases are not in physical contact.

The template synthesis of metal-semiconductor nanoparticles is relatively simple and leads to uniformly oriented particles which possess the optical properties associated with their metal and semiconductor components. UV/visible spectra calculated from theory are in qualitative accord with experiment, though further studies will be necessary to discern the effects of metal-semiconductor phase interaction. Second harmonic generation studies on these composites are also in progress.

**Acknowledgment.** The authors are grateful to the National Science Foundation for its support of this work (Grant DMR 9625151). The electron microscopy facility support was provided by the Lombardi Cancer Center Microscopy and Imaging Shared Resource (U.S. Public Health Service Grant 2P30-CA-51008).

CM980414F

(22) Bedikyan, L. D.; Miloslavskii, V. K.; Ageev, L. A. *Opt. Spektrosk.* **1979**, *47*, 225.

(23) AgI is known to be polymorphic and exists at room temperature in an equilibrium among the cubic zinc blend ( $\gamma$ -AgI) and hexagonal wurtzite ( $\beta$ -AgI) and cubic forms.

(24) (a) Kuhnke, K.; Becker, R.; Epple, M.; Kern, K. *Phys. Rev. Lett.* **1997**, *79*, 3246. (b) Alivisatos, A. P.; Waldeck, D. H.; Harris, C. B. *J. Chem. Phys.* **1985**, *82*, 541.

(25) Hornyak, G. L.; Patrissi, C. J.; Martin, C. R. *J. Phys. Chem. B* **1997**, *101*, 1548.